*Journal of Engineering Physics and Thermophysics, Vol. 82, No. 3, 2009*

# COMPARATIVE ANALYSIS OF THE FORMATION MECHANISMS OF POLYCYCLIC AROMATIC HYDROCARBONS AND FULLERENES IN FLAMES

**G. Ya. Gerasimov**

UDC 662.612

*Various formation mechanisms of polycyclic aromatic hydrocarbons and fullerenes in benzene flames have been analyzed. It has been shown that the process of building-up of the aromatic structure of the given components in the flame includes both the addition of acetylene molecules with subsequent intramolecular restructuring and formation of new aromatic rings and coagulation in which fullerenes are assembled from different aromatic fragments. We propose an optimal model of the process providing the best agreement with the available experimental data.*

***Keywords:*** *flames, aromatic hydrocarbons, fullerenes, kinetic model, combustion.*

The investigation of the formation of polycyclic aromatic hydrocarbons (PAHs) in flames is one of the main directions in the chemistry of combustion and pyrolysis of hydrocarbon fuels [1]. The interest in the problems is primarily determined by the ecological requirements for power plants, according to which the release of harmful substances into the atmosphere should comply with adopted standards. Many PAHs have high cancerogenic and mutagenic activity [2] and cause photochemical smogs in cities [3]. The presence of PAHs in combustion products leads to the formation of carbon on the working surfaces of power plants, which may lead to a decrease in the efficiency of their operation [4].

Most PAHs molecules are planar, two-dimensional (2D) aromatic compounds consisting of condensed benzene rings. *Peri*-condensed PAHs molecules with a relatively open structure contain a larger number of hydrogen atoms than *circum*-PAHs molecules in which the outer boundary is closed by five-membered rings [5]. The so-called "aromers" consisting of PAHs blocks have a bent 3D structure and can be considered as precursors of fullerenes in hydrocarbon flames [6].

The fullerenes first synthesized in laser evaporation of graphites [7] represent hollow closed shells of spherical or more complex 3D form constructed from hexa- and pentagonal carbon cells ($C_{2n}$, $n \geq 15$). The uniqueness of the structure of these carbon formations determines their unusual physical and chemical properties, holding much promise for practical applications [8]. At present, the field of application of fullerenes includes superconductors [9], catalysts [10], optical and electronic devices [11], polymers and polymer composites [12, 13], biological and medical materials [14], etc.

The methods of obtaining fullerenes of other carbon nanoparticles are rather versitile and, in particular, they include arc discharge in the blanket of inert gas with the use of graphite electrodes [15], laser irradiation of the graphite surface [16], decomposition of hydrocarbons on the surface of a metallic catalyst (CVD method) [17], laser pyrolysis of hydrocarbons [18], combustion of aliphatic and aromatic hydrocarbons at large fuel excess coefficients [19], pyrolysis of hydrocarbons in an arc plasma-jet reactor of atmospheric pressure [20], etc. Among the methods of physical action on a gas leading to the formulation of higher PAHs and fullerenes is also ionizing radiation [21]. For instance, in electron-beam cleaning of gases from harmful impurities an increase in the concentration of benz(a)pyrene, coronene, and some other PAHs is observed [22, 23].

The construction of kinetic mechanisms for complex chemically reacting systems usually includes comparison of model calculations with experimental data. At the present time, there is a large body of experimental information suitable for testing kinetic models of the formation of higher PAHs and fullerenes at combustion of aliphatic and aro-

Institute of Mechanics, M. V. Lomonosov Moscow State University, 1 Michurinskii Ave., Moscow, 119192, Russia; email: gerasimov@imec.msu.ru. Translated from Inzhenerno-Fizicheskii Zhurnal, Vol. 82, No. 3, pp. 438–447, May–June, 2009. Original article submitted April 21, 2008.

 

matic hydrocarbons [5, 24–29]. This information includes the concentration and temperature profiles obtained with the use of the GC-MS and MB-MS methods of analysis of the corresponding flames.

The last few years have seen a considerable progress in understanding the mechanisms of the formation and further growth of PAHs up to fullerenes [30, 31]. A fairly detailed review of the kinetic models is presented in [32]. Nevertheless, the existing models do not give a good description of the process under consideration. In particular, the concentration curves of fullerenes $C_{60}$ and $C_{70}$ calculated with the help of the detailed kinetic model of [31] are two orders of magnitude lower than the measured concentration. The aim of the present work is to analyze the existing formation mechanisms of higher PAHs and fullerenes and choose the most optimal kinetic model giving the best agreement with the available experimental data.

**Formation Mechanism of PAHs.** Multiple experimental data show that the formation and further transportation of PAHs upon combustion of hydrocarbon fuels is a complex multistage process closely connected with the general kinetic mechanism of combustion. The most important intermediate combustion product from the point of view of the formation of PAHs is acetylene formed due to the high-temperature oxidation of any hydrocarbon fuels [33].

The kinetic scheme of the process includes the following main stages: 1) combustion of the initial fuel with acetylene formation; 2) formation of larger molecules and radicals and, finally, of small aromatic molecules; 3) growth of aromatic molecules due to the addition to them of small acetylene molecules; 4) coagulation of PAHs molecules and radicals; 5) ion-molecular reactions. Despite the simplicity of this scheme, the structure of all stages and the role of individual elementary reactions in the general process are still not clearly understood.

The first group of reactions responsible for the combustion process is determined by the composition of the initial fuel and can be represented by kinetic models of different degrees of detailing [34]. On the one hand, these are detailed kinetic models taking into account a large number of elementary reactions and chemical components and containing enough information for describing a wide range of investigated phenomena (combustion in turbulent flow reactors and jet mixing reactors, laminar premixed flames, etc.). On the other hand, in calculating complex gas-dynamic flows when the computational difficulties make it impossible to include in the consideration a detailed kinetic model, simplified kinetic models are used.

The formation of the first aromatic ring in a chemically reacting system containing thermal decomposition products of the initial fuel includes reactions of addition of an acetylene molecule to radicals $n$–$C_4H_3$ and $n$–$C_4H_5$ with the formation, respectively, of a phenyl radical and a benzene molecule, as well as a recombination of propargyl radicals $C_3H_3$ formed under interaction between acetylene molecules and methylene radicals [33]. The latter channel, as recent investigations have shown [35], is dominating. In considering the combustion in the benzene/oxygen system, the given group of reactions can be ignored.

The further growth of PAHs is associated with the interaction of aromatic radicals with acetylene molecules. The process is described by the so-called HACA mechanism (H-abstraction-$C_2H_2$-addition) [33] which, on the one hand, is a simplification of the kinetic mechanism of growth of the aromatic structure of PAHs molecules and, on the other hand, it represents fairly exactly the main steps of the formation of aromatic rings: detachment of an H atom under interaction of an aromatic molecule $A_n$ with hydrogen atoms, and further addition of $C_2H_2$ to the aromatic radical $R_n$ formed. Destruction of aromatic molecules and radicals occurs under their interaction with O atoms and $O_2$ molecules, respectively.

It should be noted that five-membered rings are important elements of some PAHs. In particular, all fullerenes, except for hexagonal carbon cells, contain 12 pentagonal cells [36]. One of the main formation mechanisms of aromatic molecules containing five-membered rings (aryl-5) is the oxidation of six-membered aromatic rings (aryl-6) in oxy-PAHs (aryl-6-O) under their interaction with $O_2$ and the subsequent decomposition of aryl-6-O into aryl-5 and CO [37]. The further interaction of aryl-5 with acetylene forms PAHs with an odd number of C atoms in the molecule.

The coagulation mechanism describes the interaction between two PAHS particles (molecule/radical + radical) with the formation of a PAH dimer (C–C bond between two particles) with subsequent dehydrogenatiton of the dimer and closing of the ring [36]. On the basis of the structural similarity of PAHs particles for the rate constants of reactions the corresponding values for reactions benzene + phenyl [38] and phenyl + phenyl [39] were chosen as standard ones. Since the activation energies for these types of reactions are approximately equal, the pre-exponential factors in the rate constants were corrected towards higher values in accordance with the increase in the frequency of collisions $\nu \sim d^2(8\pi RT/\mu)^{1/2}$ for heavier PAHs particles than benzene [40]. If for the relation $d_n/d_6$ the expression $d_n/d_6$ =

TABLE 1. Kinetic Model of the Growth of the Structure of PAHs Particles in Hydrocarbon Flames

| Reaction | log $A$ | $E/R$, K | Lit. source |
|---|---|---|---|
| | *HACA-mechanism* | | |
| $A_n + H \rightarrow R_n + H_2$ | 14.40 | 8050 | [31] |
| $R_n + H_2 \rightarrow A_n + H$ | 12.60 | 3970 | [48] |
| $R_n + C_2H_2 \rightarrow A_{n+2} + H$ | 13.60 | 5080 | [31] |
| $R_n + C_2H_2 \rightarrow R_{n+2}$ | 13.60 | 5080 | [31] |
| $R_n + O_2 \rightarrow A_{n-2} + HCO + CO$ | 12.32 | 3760 | [30] |
| $R_n + H \rightarrow A_n$ | 14.34 | — | [49] |
| | *Coagulation mechanism* | | |
| $R_m + R_n \rightarrow A_{m+n}$ | 13.14 | 56 | [39] |
| $R_m + A_n \rightarrow A_{m+n} + H$ | 11.98 | 2170 | [38] |
| $A_{m+n} + H \rightarrow R_m + A_n$ | 13.61 | 4420 | [38] |
| | *Ion-molecular mechanism* | | |
| $H_3O^+ + A_n \rightarrow R_n^+ + H_2O$ | 14.90 | — | [45] |
| $R_n^+ + e \rightarrow A_n + H$ | 16.86 | –945 | [45] |
| $A_n^+ + C_2H_2 \rightarrow A_{n+2}^+$ | 14.75 | — | [46] |

Note. The rate constant $k = A \exp(-E/RT)$.

$0.816n^{1/2} - 1$ is taken, then the correction factor $f_{mn}$ for the coagulation rate constant of two heavy PAHs particles can be written in the form

$$f_{mn} = [0.408\,(m^{1/2} + n^{1/2}) - 1]^2\,[12/(m+n)]^{1/2}\,.$$

Unlike the general coagulation mechanism, in the so-called *zipper*-mechanism the bimolecular interaction of two PAHs particles is accompanied by the splitting-out from their periphery of several hydrogen atoms. In so doing, simultaneously several C–C bonds and the corresponding number of pentagonal and hexagonal cells are formed [41].

The zipper-mechanism plays an important part in the formation of fullerenes [32, 36]. The process begins with the formation of sandwich-like configuration of two peri-condensed PAHs molecules. The dehydrogenation of peripheral C atoms leads to the establishment between them of C–C bonds forming 12 pentagonal cells independent of the size of molecules provided they are larger than or equal to coronene ($C_{24}H_{12}$). Simultaneously with the formation of pentagonal cells their localization in energetically better positions occurs [41].

In estimating the kinetic parameters of the *zipper*-mechanism, it is necessary to take into account that with increasing mass of PAHs radicals the difference in their behavior, as compared to the behavior of molecules of the same structure, disappears [5]. While for the pairs phenyl/benzene and nephthyl/naphthalene a much lower concentration of radicals and its later maximum are observed, the concentration curves of large PAHs radicals practically do not differ from the corresponding curves for PAHs molecules. Therefore, it may be suggested that the differences in reactivities between large PAHs radicals and molecules of equal structure at high temperatures are also insignificant [25].

An important role in the formation of higher PAHs and fullerenes can be played by ion-molecular reactions [42]. Charged components are formed practically in all hydrocarbon flames, with the concentration of aromatic ions being about four orders of magnitude lower than the concentration of neutral PAHs of the same structure [5, 25, 28, 43]. The appearance of charged components in the flames is associated in the first place with the chemiionization reaction: $CH + O \rightarrow CHO^+ + e$ [42] with subsequent charge exchange of $CHO^+$ on water molecules: $CHO^+ + H_2O \rightarrow H_3O^+ + CO$ [44]. The formation of positively charged aromatic ions $PAH^+$ occurs as a result of the charge exchange of $H_3O^+$ on the corresponding PAHs molecules [45].

The further behavior of aromatic $PAH^+$ ions is only roughly understood because of the lack of kinetic formation. The main channel of growth of the structure of $PAH^+$ is the reaction of addition of $C_2H_2$ to the aromatic radical with a rate constant exceeding by two orders of magnitude the corresponding value for the addition of $C_2H_2$ to the PAHs radical [46]. Kinetic data on the coagulation of PAHs ions and molecules are practically absent. The rate constant of the dimerization reaction of $C_6H_6^+$ and $C_6H_6$ measured at temperatures close to room temperature and at a

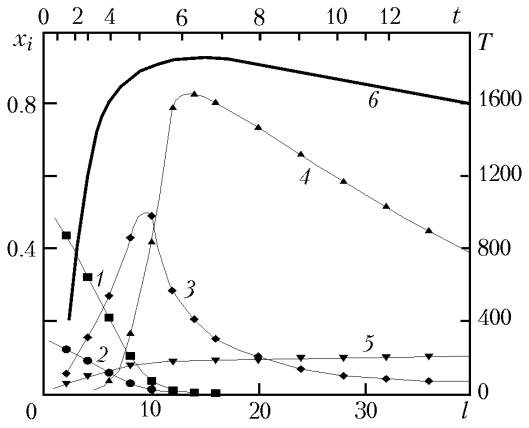


Fig. 1. Molar fractions of components $x_i$ (1–5) and temperature $T$ (6) depending on the distance to the burner $l$ and the process time $t$ in the benzene/oxygen flame: 1) $O_2$; 2) $C_6H_6$; 3) $C_2H_2$ ($x_i \cdot 10$); 4) H ($x_i \cdot 10^2$; 5) $H_2$. $T$, K; $t$, msec; $l$, mm.

pressure $p$ = 0.1 Pa [47] is about two orders of magnitude lower than the corresponding value for the dimerization of phenyl radicals [39].

The table shows the simplified kinetic model of the growth of PAHs particles in hydrocarbon flames including the above-described kinetic mechanism. In performing calculations, the model was corrected on the basis of comparison of the obtained results with the available experimental data. A detailed description of the changes made with corresponding comments is given below.

**Computational Procedure.** Analysis of the formation mechanisms of PAHs and fullerenes was carried out on the basis of comparison of the calculated concentration curves with the experimental ones with the example of a laminar, one-dimensional, premixed benzene flame with axial diffusion: C/O = 0.80, the gas velocity in the burner $v$ at a temperature $T$ = 298 K is 0.42 m/sec, $p$ = 2.66 kPa [5, 28]. Since the considered PAHs components are high-molecular compounds, their diffusion coefficients are much lower than the corresponding values for the light components of the flame. Therefore, it may be suggested that the diffusion effects weakly influence their concentration profiles and can be neglected. In this case, to describe the dynamics of the process of transformation of the PAHs components, we can make use of the approximation of the plug-flow reactor.

The concentration of PAHs particles in hydrocarbon flames is much smaller than the concentration of components with which they interact ($C_6H_6$, $C_2H_2$, $H_2$ molecules, H radicals, etc.) [5]. This provides the possibility of separating the kinetics of their growth and the combustion kinetics. The available experimental data contain enough information for the approximation of the concentration curves of the light components of the flame and its temperature profiles, which removes the problem of computational modeling of the combustion in the flow with account for the transfer processes, and in describing the transformation of PAHs particles makes it possible to restrict ourselves to the solution of the direct kinetic problem.

Figure 1 shows the temperature and concentrations of intermediate components of the flame benzene/oxygen (C/O = 0.72, the mass fraction of argon in the initial mixture is 30%, $v_{25^oC}$ = 0.5 m/sec, $p$ = 2.67 kPa) used in analyzing the formation mechanisms of PAHs and fullerenes [50]. The concentration profiles of $C_5H_5$ molecules and $C_5H_6$ and $C_6H_5$ radicals are given in [24, 31]. It should be noted that the characteristics of the given flame somewhat differ from the above characteristics of the flame in which the concentrations of PAHs molecules, radicals, and ions were measured [5, 28]. Nevertheless, the concentration curves of the main components in these two flames ($C_6H_6$, CO, $CO_2$, $H_2$, $H_2O$, low-molecular hydrocarbons) do not differ widely from each other [28].

The process of formation and transformation of PAHs particles was calculated for a time up to $t_{max}$ = 20 msec. The process time uses as a reference to the distance to the burner edge along the flame axis on the basis of a comparison of the time and step scales [50] given in Fig. 1. PAHs molecules or radicals with the same number $n$ but with a different content of H atoms were considered as one component: $A_n$ or $R_n$. In the numerical realization of the

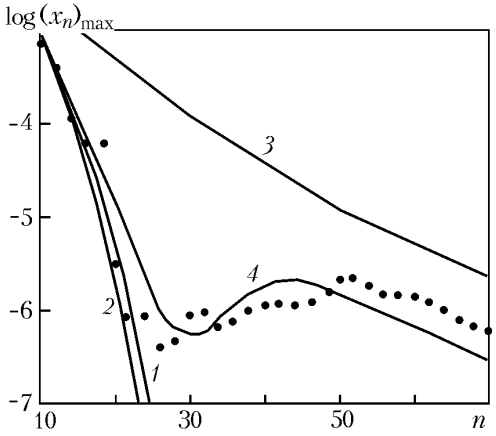


Fig. 2. Maximum concentrations of PAHs molecules with an even number of C atoms as a function of n. Results of calculations: 1) HACA mechanism; 2) HACA mechanism + coagulation mechanism; 3) HACA mechanism + coagulation mechanism without account for inverse reactions; 4) recommended mechanism. Dots show the experimental data of [5].

coagulation mechanism, the $n$ value was varied from 5 to 90, and the $m$ value was varied from $n$ to 90 (see the corresponding reactions given in the table).

**Results and Discussion.** To estimate the contribution of different mechanisms on the formation dynamics of PAHs and fullerenes, a series of calculations has been performed. In Fig. 2, the results of the calculation of maximum concentrations of PAHs molecule with an even number of C atoms in a molecule are compared to the experimental data of [5]. As is seen, the HACA-mechanism (curve 1) gives a good agreement between the calculated and measured concentrations $(x_n)_{max}$ only at $n \le 24$. The experimental values of $(x_n)_{max}$ at $20 \le n \le 70$ remain at a level of about $10^{-6}$, whereas the calculated values decrease sharply with increasing $n$. This can be due to the fact that in the considered flame at $l \ge 10$ mm there is a decrease in the concentration of $C_2H_2$ by more than an order of magnitude compared to its maximum value (see Fig. 1), which in calculating by the HACA mechanism leads to a corresponding decrease in the rate of formation of large aromatic molecules.

Building-up of the aromatic structure in the HACA mechanism presupposes a sequential increase in the mass of molecules under their interaction with acetylene molecules and, accordingly, a later appearance in the flame of heavy PAHs components. Nevertheless, the experimental data show that heavier PAHs molecules can appear in the flame at earlier stages of the process than light ones [51]. This indicates that the HACA-mechanism does not provide an adequate description of the process of formation of higher PAHs.

Including in consideration the coagulation mechanism leads to some decrease in the concentrations $(x_n)_{max}$ (curve 2 in Fig. 2). This somewhat unexpected result can be explained by the reaction inverse to the coagulation reaction: $A_{m+n} + H \rightarrow R_m + A_n$ (see the table) which has a dominant role in the formation and decomposition of biphenyl [38]. The interaction of two PAHs particles can lead, on the one hand, to the formation of biaryl (one C–C bond between two reagents) which then either decomposes into the initial components in the inverse reaction or, as a result of the internal restructuring, transforms into a more stable aromatic compound with the formation of a new ring [52]. On the other hand, in the *zipper* variety of the coagulation mechanism several C–C bonds between interacting PAHs particles appear simultaneously, which directly forms a stable aromatic molecule $A_{m+n}$ without the formation of an intermediate biaryl compound. The interaction of this molecule with an H atom leads not to its decomposition into the initial components but to the formation of an aromatic radical in the reaction $A_{m+n} + H \rightarrow R_{m+n} + H_2$ (see HACA mechanism in the table). Nevertheless, an attempt to completely exclude the considered inverse reaction from the kinetic scheme gives values of the maximum concentration $(x_n)_{max}$ in the range $20 \le n \le 70$ higher by one-two orders of magnitude (curve 3 in Fig. 2).

The analysis performed makes it possible to distinguish the main features of the real formation mechanism of PAHs in benzene flames. This is, firstly, the ability of the HACA mechanism to describe the behavior of aromatic components only for $n \le 24$. Secondly, the coagulation mechanism in its irreversible form (*zipper*-mechanism)

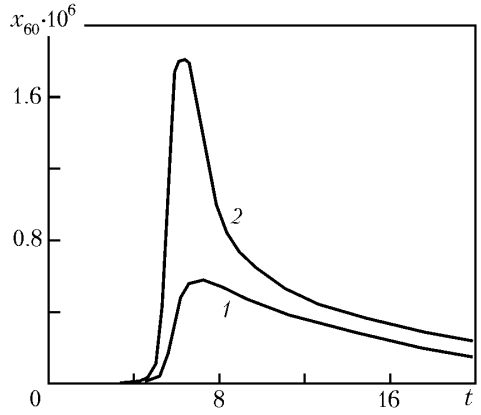


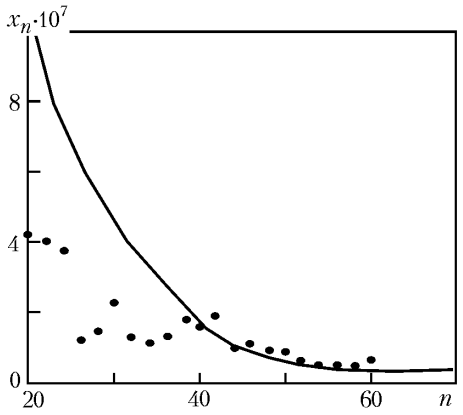


Fig. 3. Concentration of fullerenes $C_{60}$ versus the process time at various maximum temperatures in the flame: 1) $T_{max}$ = 1950 K; 2) 2250. $t$, msec.

Fig. 4. Concentration of PAHs molecules with an even number of C atoms depending on $n$: dots show the experimental data of [5] at $l$ = 7 mm, the curve presents the results of calculations at $t$ = 5 msec.

begins to work at $n \geq 20$. As mentioned above, the difference in reactivities between large PAHs radicals and molecules of equal structure at high temperatures are insignificant [25]. Therefore, the kinetic model of the growth of the structure of PAHs particles with large $n$ values should contain the coagulation of aromatic molecules with a rate constant equal to the corresponding value for the coagulation of aromatic radicals. As calculations show, the best agreement with experimental data for the quantity $(x_n)_{max}$ is reached taking into account the coagulation of aromatic molecules having $n \geq 16$.

Thus, the recommended formation mechanism of PAHs is benzene flames includes the HACA mechanism and the coagulation mechanism in which decomposition of the molecule $A_{m+n}$ under its interaction with an H atom occurs only at $m + n \leq 20$ and coagulation of aromatic molecules begins at $n$ = 16. The results of the calculation on the basis of the given mechanism are presented by curve 4 in Fig. 2. It is seen that in general the calculation data follow the behavior of the experimental points. In the range of large $n$ values ($50 \leq n \leq 70$), the calculated values of the quantity $(x_n)_{max}$ are about twice lower than the measured ones.

It should be noted that in the considered kinetic model the PAHs components differ only in the content of C atoms in the aromatic particle without concrete definition of its internal structure and, accordingly, of the number of H atoms. This imposes certain restrictions on the practical use of results obtained with the aid of the model. Nevertheless, the existing detailed kinetic models that consider in detail the growth of PAHs particles are unable to catch all essential details of the given process. In particular, the fairly perfect model developed in [31] gives a satisfactory agreement with experimental data only for compounds with $n \leq 20$. The calculated concentrations of fullerenes $C_{60}$ and $C_{70}$ are about two orders of magnitudes lower than their measured values.

The formation of fullerenes $C_{60}$ and $C_{70}$ in the proposed kinetic model is a part of the general process of growth of the aromatic structure of PAHs particles in which both the addition of acetylene molecules with subsequent intramolecular restructuring and the formation of new aromatic rings and the coagulation are taken into account. Unlike the known kinetic model [36] where the coagulation channel of the fullerene $C_{60}$ formation takes into account only the reaction $C_{30} + C_{30} \rightarrow C_{60}$, in the given kinetic model fullerenes are assembled from various aromatic fragments in accordance with the general ideas about the character of the given process [53].

Figure 3 shows the dependence $x_{60} = x_{60}(t)$ calculated for various maximum temperatures in the flame. As mentioned above, the initial data for the calculation (concentrations of the main components and the temperature profile) were taken for the benzene/oxygen flame [50] whose parameters differ somewhat from the characteristics of the flame in which the concentrations of PAHs molecules and radicals were measured [5]. In particular, the maximum temperature in the flame in [5] is higher by 300 K and equals $T_{max}$ = 2250 K. As is seen from Fig. 3, the concentration of fullerenes $x_{60}$ increases sharply in the portion of the flame where its maximum temperature is reached and

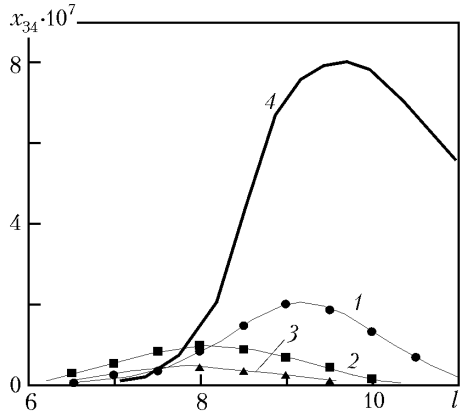


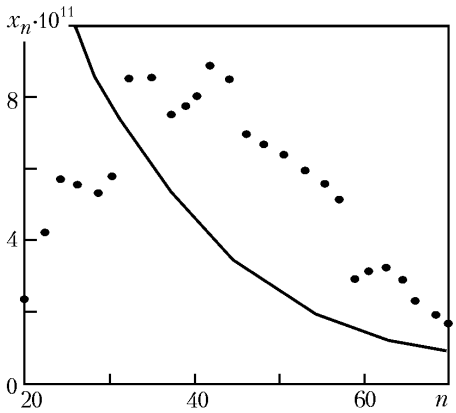


Fig. 5. Concentration of $C_{34}$ and its components depending on the distance to the burner edge: dots show the experimental data of [5]: 1) $C_{34}H_{14}$; 2) $C_{34}H_{16}$; 3) $C_{34}H_{18}$; curve 4 presents the results of the calculation of the total concentration of $C_{34}$. $l$, mm.

Fig. 6. Concentrations of molecular ions $PAH^+$ with an even number of C atoms depending on $n$: dots show the experimental data of [28] at $l$ = 9 mm; the curve presents the results of calculations at $t$ = 5.2 msec.

then decreases smoothly by about one order of magnitude at $t$ = 20 msec, which agrees qualitatively with the available experimental data [27].

Figure 4 compares the results of calculations of the concentrations of PAHs molecules with an even number of C atoms with the experimental data of [5]. On average, higher calculated data at $20 \le n \le 40$ and their lower values at $n > 40$ are observed, which agrees with the general trend of curve 4 in Fig. 2. The behavior of the calculated dependences $x_n = x_n(t)$ follows the observed behavior of $x_n$ along the jet axis. These values pass through the maximum within the limits of the fuel oxidation zone and then decrease so that in the combustion products the content of higher PAHs is insignificant. The distance $l$ from the burner edge at which the maximum of $x_n$ is reached increases, on average, with increasing $n$ and is in the 9–12 mm range, which agrees with the experimental data of [5]. A typical profile of $x_n = x_n(t)$ is given in Fig. 5.

The formation of aromatic ions $PAH^+$ was calculated at a given distribution of the $H_3O^+$ concentration along the jet axis [44] on the assumption that $PAH^+$ concentrations are much smaller than the concentration of $H_3O^+$. The maximum value of the mole fraction of $H_3O^+$ reached at $l$ = 8 mm was taken to be equal to $10^{-8}$ [28]. Despite the fact that in the hydrocarbon flames the concentration maximum of negative ions is shifted (due to the diffusion effects) relative to the maximum of positive ions towards the burner [42], it is believed that the concentration of negative ions (electrons) at each instant of time is equal to the $H_3O^+$ concentrations.

In Fig. 6, the results of the calculation of concentrations of $PAH^+$ ions with an even number of C atoms are compared to the experimental data of [28]. The calculation curve was obtained with the use of only the mechanism of charge exchange of $H_3O^+$ on the corresponding PAHs molecules and subsequent recombination of $PAH^+$ and electrons. As is seen from the table, the rate constant of the reaction of addition of $C_2H_2$ to the aromatic radical at $T \approx 2000$ K exceeds by two orders of magnitude the corresponding value for the addition of $C_2H_2$ to the PAHs radical. Therefore, account of the ion-molecular mechanism of $PAH^+$ growth in the computational algorithm leads to a fast equalization of $PAH^+$ concentrations at a level of $x_n(PAH^+) = 10^{-9}$. From this it follows that the given rate constant is at least one order of magnitude higher.

## CONCLUSIONS

1. The recommended formation mechanism of PAHs in benzene flames includes the HACA mechanism and the coagulation mechanism. In the irreversible *zipper* kind of coagulation mechanism, the number of C atoms in the

formed particle should exceed 20, and coagulation of aromatic molecules takes place for molecules with a number of atoms C greater than 16.

2. The formation of fullerenes is a part of the general process of growth of the aromatic structures of PAHs particles taking into account both the addition of acetylene molecules with subsequent intramolecular restructing and formation of new aromatic rings and the coagulation in which fullerenes are assembled from different aromatic fragments.

3. The results obtained can be used in constructing kinetic models of the formation of polycyclic aromatic hydrocarbons and fullerenes in hydrocarbon gases under different physical actions on the gas, in particular, under the action of ionizing radiation.

Part of this work was supported by the IAEA (International Atomic Energy Agency, Research Contract No. F23024/13139).

## NOTATION

$A$, pre-exponential factor in the reaction rate constant, $cm^3 \cdot mole^{-1} \cdot sec^{-1}$; $A_n$, aromatic molecule containing $n$ C atoms; $d$, molecule diameter, m; $E$, activation energy of the reaction, J/mole; $f$, correction factor to the coagulation rate constant; $k$, reaction rate constant, $cm^3 \cdot mole^{-1} \cdot sec^{-1}$; $l$, distance from the burner along the flame axis, m; $m$, $n$, number of A atoms in the aromatic particle; $p$, pressure, Pa; $R$ = 8.31 J/(mole·K), universal gas constant; $R_n$, aromatic radical containing $n$ C atoms; $T$, temperature, K; $t$, time, sec; $v$, gas velocity, m/sec; $x_i$, molar fraction of the $i$th gas component; $x_n$, molar fraction of aromatic particles containing $n$ C atoms; $\mu$, reduced mass of two colliding gas particles, kg; $\nu$, collision frequency, $sec^{-1}$. Subscripts: $i$, component number; max, maximum value.

## REFERENCES5

1. J. M. Simmie, Detailed chemical kinetic models for the combustion of hydrocarbon fuels, *Prog. Energy Combust. Sci.*, **29**, No. 6, 599–634 (2003).
2. J. Durant, W. F. Busby, A. L. Lafleur, B. W. Penman, and C. L. Crespi, Human cell mutagenicity of oxygenated, nitrated and unsubstituted polycyclic aromatic hydrocarbons associated with urban aerosols, *Mutat. Res.*, **371**, Nos. 3–4, 123–157 (1996).
3. N. Tang, T. Hattori, R. Taga, K. Igarashi, X. Yang, K. Tamura, H. Kakimoto, V. F. Mishukov, A. Toriba, R. Kizu, and K. Hayakawa, Polycyclic aromatic hydrocarbons and nitropolycyclic aromatic hydrocarbons in urban air particulates and their relationship to emission sources in the Pan-Japan Sea countries, *Atmos. Environ.*, **39**, No. 32, 5817–5826 (2005).
4. L. Maurice and T. Edwards, Liquid hydrocarbon fuels for hypersonic propulsion, in: E. T. Curran and S. N. B. Murthy (Eds.), *Scramjet Propulsion*, *Progress in Astronautics and Aeronautics*, Reston: *AIAA*, **189**, 757–822 (2000).
5. A. Keller, R. Kovacs, and K.-H. Homann, Large molecules, ions, radicals and small soot particles in fuel-rich hydrocarbon flames. Pt. IV. Large polycyclic aromatic hydrocarbons and their radicals in a fuel-rich benzene–oxygen flame, *Phys. Chem. Chem. Phys.*, **2**, No. 8, 1667–1675 (2000).
6. M. Bachmann, W. Wiese, and K.-H. Homann, PAH and aromers: Precursors of fullerenes and soot, *Symp.* (*Int.*) *on Combust.*, **26**, No. 2, 2259–2267 (1996).
7. H. W. Kroto, J. R. Heath, S. C. O'Brien, R. F. Curl, and R. E. Smalley, $C_{60}$: Buckminsterfullerene, *Nature*, **318**, No. 6042, 162–163 (1985).
8. I. P. Suzdalev, *Nanotechnology: Physics and Chemistry of Nanoclusters*, *Nanostructures*, *and Nanomaterials* [in Russian], Kom-Kniga, Moscow (2006).
9. J. L. Margrave, $C_{60}$, $C_{70}$ and other fullerenes: A new class of materials yields versatile organic superconductors, *Appl. Supercond.,* **1**, Nos. 7–9, 867–868 (1993).
10. S.-F. Zhang, J. R. Shearman, M. Domin M., M.-J. Lazaro, A. A. Herod, and R. Kandiyoti, Catalytic activity of fullerenes for hydrocracking coal extracts, *Fuel*, **76**, No. 3, 207–214 (1997).
11. A. Al-Mohamad and A. W. Allaf, Fullerene-60 thin films for electronic applications, *Synth. Met.*, **104**, No. 1, 39–44 (1999).

12. A. O. Patil and S. J. Brois, Fullerene grafted hydrocarbon polymers, *Polymer*, **38**, No. 13, 3423–3424 (1997).
13. C.-C. Wang, Z.-X. Guo, S. Fu, W. Wu, and D. Zhu, Polymers containing fullerene or carbon nanotube structures, *Prog. Polym. Sci.*, **29**, No. 11, 1079–1141 (2004).
14. A. W. Jensen, S. R. Wilson, and D. I. Schuster, Biological application of fullerenes, *Bioorg. Med. Chem.*, **4**, No. 6, 767–779 (1996).
15. N. I. Alekseyev and G. A. Dyuzhev, Fulllerene formation in an arc discharge, *Carbon*, **41**, No. 7, 1343–1348 (2003).
16. D. Kasuya, F. Kokai, K. Takahashi, M. Yudasaka, and S. Iijima, Formation of $C_{60}$ using $CO_2$ laser vaporization of graphite at room temperature, *Chem. Phys. Lett.*, **337**, Nos. 1–3, 25–30 (2001).
17. S. Musso, S. Porro, M. Rovere, M. Giorcelli, and A. Tagliaferro, Fluid dynamic analysis of gas flow in a thermal-CVD system designed for growth of carbon nanotubes, *J. Cryst. Growth*, **310**, No. 2, 477–483 (2007).
18. S. Petcu, M. Cauchetier, X. Armand, I. Voicu, and R. Alexandrescu, Formation of fullerenes in the laser pyrolysis of benzene, *Combust. Flame*, **122**, No. 4, 500–507 (2000).
19. H. Takehara, M. Fujiwara, M. Arikawa, M. Diener, and J. M. Alford, Experimental study of industrial scale fullerene production by combustion synthesis, *Carbon*, **43**, No. 2, 311–319 (2005).
20. A. F. Bublievskii, A. A. Galinovskii, A. V. Gorbunov, S. A. Zhdanok, L. I. Sharakhovskii, and A. L. Mossé, Plasma pyrolytic synthesis of carbon nanostructures in a mixture of nitrogen and propane–butane, *Inzh.-Fiz. Zh.*, **79**, No. 2, 3–9 (2006).
21. G. Gerasimov, Modeling study of electron-beam polycyclic and nitro-polycyclic aromatic hydrocarbons treatment, *Radiat. Phys. Chem.*, **76**, No. 1, 27–36 (2007).
22. M. S. Callen, M. T. de la Cruz, S. Marinov, R. Murillo, M. Stefanova, and A. M. Mastral, Flue gas cleaning in power stations by using electron beam technology. Influence on PAH emissions, *Fuel Process. Technol.*, **88**, No. 2, 251–258 (2007).
23. A. Ostapczuk, J. Licki, and A. G. Chmielewski, Polycyclic aromatic hydrocarbons in coal combustion flue gas under electron beam irradiation, *Radiat. Phys. Chem.*, **77**, No. 4, 490–496 (2008).
24. H. Richter and J. B. Howard, Formation and consumption of single-ring aromatic hydrocarbons and their precursors in premixed acetylene, ethylene and benzene flames, *Phys. Chem. Chem. Phys.*, **4**, No. 11, 2038–2055 (2002).
25. P. Weilmünster, A. Keller, and K.-H. Homann, Large molecules, ions, radicals and small soot particles in fuel-rich hydrocarbon flames. Pt. I. Positive ions of polycyclic aromatic hydrocarbons (PAH) in low-pressure premixed flames of acetylene and oxygen, *Combust. Flame*, **116**, Nos. 1–2, 62–83 (1999).
26. A. B. Fialkov and K.-H. Homann, Large molecules, ions, radicals and small soot particles in fuel-rich hydrocarbon flames. Pt. VI. Positive ions of aliphatic and aromatic hydrocarbons in low-pressure premixed flame of *n*-butane and oxygen, *Combust. Flame*, **127**, No. 3, 2076–2090 (2001).
27. W. J. Grieco, A. L. Lafleur, K. C. Swallow, H. Richter, K. Taghizadeh, and J. B. Howard, Fullerenes and PAH in low-pressure premixed benzene/oxygen flames, *Symp.* (*Int.*) *on Combust.*, **27**, No. 2, 1669–1675 (1998).
28. A. B. Fialkov, J. Dennebaum, and K.-H. Homann, Large molecules, ions, radicals and small soot particles in fuel-rich hydrocarbon flames. Pt. V. Positive ions of polycyclic aromatic hydrocarbons (PAH) in low-pressure premixed flames of benzene and oxygen, *Combust. Flame*, **125**, Nos. 1–2, 763–777 (2001).
29. M. Bachmann, J. Griesheimer, and K.-H. Homann, The formation of $C_{60}$ and its precursors in naphthalene flames, *Chem. Phys. Lett.*, **223**, Nos. 5–6, 506–510 (1994).
30. H. Wang and M. Frenklach, A detailed kinetic modeling study of aromatics formation in laminar premixed acetylene and ethylene flames, *Combust. Flame*, **110**, Nos. 1–2, 173–221 (1997).
31. H. Richter, W. J. Grieco, and J. B. Howard, Formation mechanism of polycyclic aromatic hydrocarbons and fullerenes in premixed benzene flames, *Combust. Flame*, **119**, Nos. 1–2, 1–22 (1999).
32. H. Richter and J. B. Howard, Formation of polycyclic aromatic hydrocarbons and their growth to soot — a review of chemical reaction pathways, *Prog. Energy Combust. Sci.*, **26**, Nos. 4–6, 565–608 (2000).
33. M. Frenklach, Reaction mechanism of soot formation in flames, *Phys. Chem. Chem. Phys.*, **4**, No. 11, 2028–2037 (2002).

34. G. Ya. Gerasimov and S. A. Losev, Kinetic models of combustion of kerosene and its components, *Inzh.-Fiz. Zh.*, **78**, No. 6, 14–25 (2005).
35. R. X. Fernandes, H. Hippler, and M. Olzmann, Determination of the rate coefficient for the $C_3H_3 + C_3H_3$ reaction at high temperatures by shock-tube investigations, *Proc. Combust. Inst.*, **30**, No. 1, 1033–1038 (2005).
36. C. J. Pope, J. A. Marr, and J. B. Howard, Chemistry of fullerenes $C_{60}$ and $C_{70}$ formation in flames, *J. Phys. Chem.*, **97**, No. 42, 11001–11013 (1993).
37. N. Kunioshi, M. Touda, and S. Fukutani, Computational study on the formation of five-membered rings in PAH through reaction with $O_2$, *Combust. Flame*, **128**, No. 3, 292–300 (2002).
38. J. Park, S. Burova, A. S. Rodgers, and M. C. Lin, Experimental and theoretical studies of the $C_6H_5 + C_6H_6$ reaction, *J. Phys. Chem. A*, **103**, No. 45, 9036–9041 (1999).
39. J. Park and M. C. Lin, Kinetics for the recombination of phenyl radicals, *J. Phys. Chem. A*, **101**, No. 1, 14–18 (1997).
40. H. Richter, S. Granata, W. H. Green, and J. B. Howard, Detailed modeling of PAH and soot formation in laminar premixed benzene/oxygen/argon low-pressure flame, *Proc. Combust. Inst.*, **30**, No. 1, 1397–1405 (2005).
41. J. Ahrens, M. Bachmann, Th. Baum, J. Griesheimer, R. Kovacs, P. Weilmünster, and K.-H. Homann, Fullerenes and their ions in hydrocarbon flames, *Int. J. Mass Spectrom. Ion Process*, **138**, No. 1, 133–148 (1994).
42. A. B. Fialkov, Investigation on ions in flames, *Prog. Energy Combust. Sci.*, **23**, Nos. 5–6, 399–528 (1997).
43. Ph. Gerhardt and K.-H. Homann, Ions and charged soot particles in hydrocarbon flames. III. Negative ions in fuel-rich acetylene/oxygen flames, *Ber. Bunsenges. Phys Chem.*, **94**, No. 10, 1086–1096 (1990).
44. J. Prager, U. Riedel, and J. Warnatz, Modeling ion chemistry and charged species diffusion in lean methane-oxygen flames, *Proc. Combust. Inst.*, **31**, No. 1, 1129–1137 (2007).
45. J. Woodal, M. Agundez, A. J. Markwick, and T. J. Millar, The UMIST database for astrochemistry, *Astronomy Astrophys.*, **466**, No. 3, 1197–1204 (2007).
46. H. F. Calcote and R. J. Gill, Comparison of the ionic mechanism of soot formation with a free radical mechanism, in: H. Bockhorn (Ed.), *Soot Formation in Combustion. Mechanisms and Models*, *Springer Series in Chemical Physics*, Vol. 59, Springer, Berlin (1994), pp. 471–484.
47. S. Lui, F. Jarrold, and M. T. Bowers, Ion-molecule clustering in simple systems. A study of the temperature dependence of the dimerization reactions of $CH_2CF_2^+$, $C_6H_6^+$ (benzene), and $C_6D_6^+$ (benzene-$d_6$) in the parent neutral gases: experiment and theory, *J. Phys. Chem.*, **89**, No. 14, 3127–3134 (1985).
48. E. Heckmann, H. Hipper, and J. Troe, High-temperature reactions and thermodynamic properties of phenyl radicals, *Symp.* (*Int.*) *on Combust.*, **26**, No. 1, 543–550 (1996).
49. S. G. Devis, H. Wang, K. Brezinsky, and C. K. Law, Laminar flame speeds and oxidation kinetics of benzene–air and toluene–air flames, *Symp.* (*Int.*) *on Combust.*, **26**, No. 1, 1025–1033 (1996).
50. J. D. Bittner, J. B. Howard, and H. B. Palmer, Chemistry of intermediate species in the rich combustion of benzene, in: J. Lahaye and G. Prado (Eds.), *Soot in Combustion Systems and Its Toxic Properties*, Plenum Press, New York (1983), pp. 95–125.
51. H. Hepp, K. Siegmann, and K. Sattler, New aspects of growth mechanisms for polycyclic aromatic hydrocarbons in diffusion flames, *Chem. Phys. Lett.*, **233**, No. 1, 16–22 (1995).
52. A. F. Sarofim, J. P. Longwell, M. J. Wornat, and J. Mukherjee, The role of biaryl reactions in PAH and soot formation, in: H. Bockhorn (Ed.), *Soot Formation in Combustion. Mechanisms and Models*, *Springer Series in Chemical Physics*, Vol. 59, Springer, Berlin (1994), pp. 485–499.
53. Yu. E. Lozovik and A. M. Popov, Formation and growth of carbon nanostructures: fullerenes, nanoparticles, nanotubes, and cones, *Usp. Fiz. Nauk*, **167**, No. 7, 751–774 (1997).